

Faster seafloor spreading and lithosphere production during the mid-Cenozoic

Clinton P. Conrad

Department of Earth and Planetary Sciences, Johns Hopkins University, Baltimore, Maryland 21218, USA

Carolina Lithgow-Bertelloni

Department of Geological Sciences, University of Michigan, Ann Arbor, Michigan 48109, USA

ABSTRACT

Concurrent changes in seawater chemistry, sea level, and climate since the mid-Cretaceous are thought to result from an ongoing decrease in the global rate of lithosphere production at ridges. The present-day area distribution of seafloor ages, however, is most easily explained if lithosphere production rates were nearly constant during the past 180 m.y. We examined spatial gradients of present-day seafloor ages and inferred ages for the subducted Farallon plate to construct a history of spreading rates in each major ocean basin since ca. 140 Ma, revealing dramatic Cenozoic events. Globally, seafloor spreading rates increased by ~20% during the early Cenozoic due to an increase in plate speeds in the Pacific basin. Since then, subduction of the fast-spreading Pacific-Farallon ridge system has led to a 12% decrease in average global spreading rate and an 18% or more decrease in the total rate of lithosphere production by the most conservative estimates. These rapid changes during the Cenozoic defy models of steady-state seafloor formation, and demonstrate the time-dependent and evolving nature of plate tectonics on Earth.

Keywords: ridge spreading, seafloor ages, crustal production, plate tectonics, Farallon plate.

INTRODUCTION

The motions of Earth's tectonic plates represent the surface manifestation of convection in the Earth's mantle, and, over time scales of 50–100 m.y., govern a variety of geological processes, including mantle heat loss, sea-level change (Kominz, 1984; Gaffin, 1987), the carbon cycle (Bernier and Kothavala, 2001), and seawater chemistry (Hardie, 1996). Although the basic history of plate motions has been deduced for the Cenozoic and some of the Mesozoic, controversy has emerged regarding changes in the global rates of ridge spreading and lithospheric production during this time period. Tectonic reconstructions suggest that plate velocities have increased during the Cenozoic, particularly in the Pacific (Cogné and Humler, 2004), yet global studies of rates of ridge spreading (Kominz, 1984) or subduction (Engelbretson et al., 1992) suggest that lithospheric production rates at ridges have slowed during the Cenozoic. Rowley (2002) used the area-age distribution of the present-day ocean floor to suggest that seafloor production rates have remained nearly constant since 180 Ma. This controversy has introduced questions over whether Cenozoic trends such as sea-level lowering (Haq et al., 1987), increasing Mg/Ca ratio in seawater (Hardie, 1996), and decreasing atmospheric carbon and associated cooling (Bernier and Kothavala, 2001) are the results of decreasing lithospheric production rates.

The youngest seafloor, recently produced at spreading ridges, occupies proportionally more area than does older seafloor because it is less likely to have been subducted since the time of its formation. By examining the area distribution of seafloor ages, Parsons (1982) and Rowley (2002) observed an approximately triangular shape for the distribution of area per unit age versus age. Rowley (2002) noted that this distribution is the expected result of a constant rate of seafloor production at ridges combined with consumption of seafloor with a uniform age distribution. In the absence of any other information about past seafloor production rates, the present-day seafloor age distribution gives no reason to suspect a significant change in production rates during the past 180 m.y. (Rowley, 2002). Although it ignores information about past rates that can be gleaned from tectonic plate reconstructions, Rowley's (2002) study is appealing because it relies only on well-defined (Müller et al., 1997) age data from the present-day seafloor. Other studies that infer faster production rates for past times (e.g., Kominz, 1984; Engelbretson et al., 1992) rely on tectonic reconstructions that inevitably carry a degree of uncertainty.

Maps of present-day seafloor ages (Müller et al., 1997), however, contain additional information about the spreading systems that originally formed this seafloor. For example, Cogné and Humler (2004) recognized that the spacing of isochrons provides a time history of past spreading rates. In addition, the symmetry of

seafloor spreading allows us to estimate the age distribution of subducted seafloor, the spreading counterpart of which is still preserved. We use these additional pieces of information to detect changes in spreading rate, ridge length, and seafloor production rates as functions of time and between ocean basins. Although these estimates become increasingly uncertain with age because subduction is constantly destroying information about past spreading environments, we can observe trends, particularly during the Cenozoic, that deviate from the constant spreading model suggested by the seafloor age distribution alone. As in Rowley's (2002) study, our estimates are based only on seafloor ages measured from the present-day seafloor and are thus not subject to potential uncertainty associated with reconstructions of past plate motions.

PAST SEAFLOOR SPREADING RATES AND RIDGE LENGTHS

The age of the ocean floor at any point (θ , ϕ) = (colatitude, longitude) can be determined by examining the pattern of parallel magnetic anomalies that record Earth's magnetic field at the time of their formation at a spreading ridge. By interpolating between the locations of dated magnetic anomalies and using additional information from fracture-zone traces, Müller et al. (1997) determined the seafloor age on a $0.1^\circ \times 0.1^\circ$ grid (Fig. 1A). We use it to estimate past spreading rates and ridge lengths through analysis of seafloor age gradients.

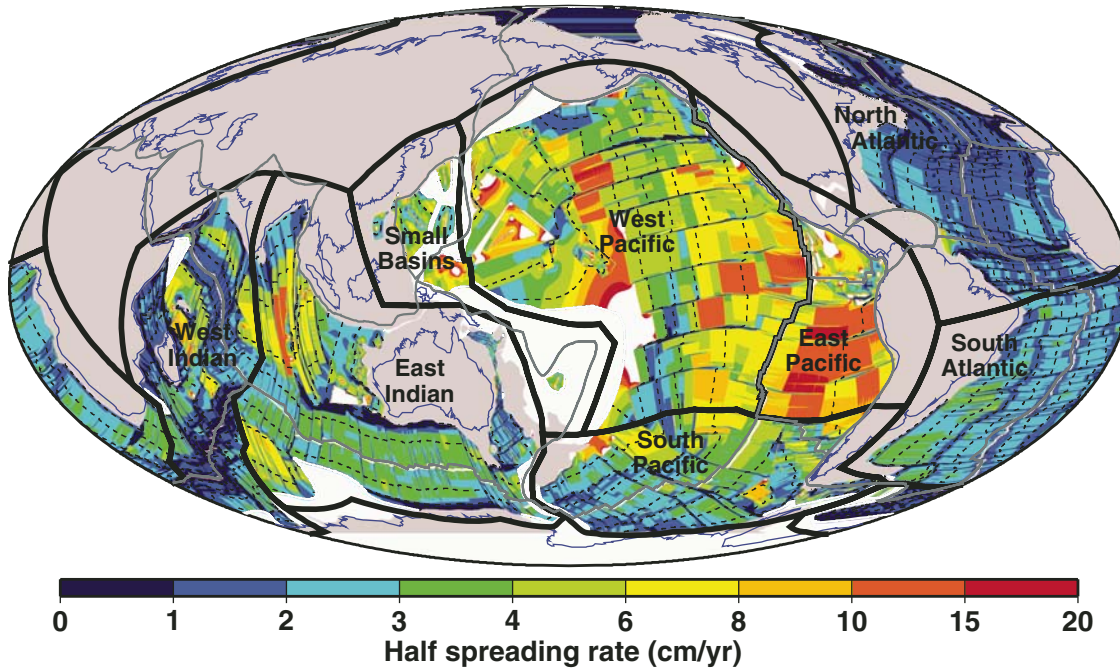


Figure 1. Half-spreading rate at time oceanic lithosphere was originally produced, as determined by applying Equation 1 to seafloor age map of Müller et al. (1997). Light gray indicates regions where ages or rates cannot be determined, middle gray indicates continental areas, and dark gray indicates plate boundaries. Dashed black lines are 25 m.y. age contours. We have defined eight different ocean basins, the boundaries of which, shown in black, are drawn through continents and along transform faults.

The gradient of seafloor age, $T(\theta, \phi)$, is inversely proportional to a rate of spreading, $v_{sp}(\theta, \phi)$:

$$v_{sp}(\theta, \phi) = \frac{R_E}{\sqrt{T(\theta, \phi)}} = R_E \left[\left(\frac{1}{\sin(\theta)} \frac{\partial T(\theta, \phi)}{\partial \phi} \right)^2 + \left(\frac{\partial T(\theta, \phi)}{\partial \theta} \right)^2 \right]^{-1/2}, \quad (1)$$

where R_E is the radius of the Earth. When applied to seafloor age data, inverse age gradients calculated using Equation 1 yield half-spreading rates that applied at the time of seafloor formation (Müller et al., 1998). We determined $v_{sp}(\theta, \phi)$ for all points with defined ages in Müller et al.'s (1997) data set (Fig. 1). Some regions, particularly within the Pacific's poorly defined mid-Cretaceous quiet zone (118–83 Ma), show anomalously fast spreading rates in excess of 20 cm/yr, which we omit from further analysis. We also ignore rates determined for seafloor younger than 1 Ma because gradients measured from such points often span the ridge, and thus do not correspond to spreading rates. Because age gradients across transform faults are large, our determination of spreading rate (Equation 1) assigns slow apparent rates near transform faults in all basins (Fig. 1). Because these slow rates are nonphysical artifacts, we remove them from further analysis, as described in the following.

The total length of preserved spreading, L_{sp} along an isochron of age t can be determined by integrating local estimates of the spreading length, dL_{sp} , over points whose ages are within an age range ΔT that is centered about t :

$$L_{sp}(t) = \int_{T(\theta, \phi) = t - \Delta T/2}^{T(\theta, \phi) = t + \Delta T/2} dL_{sp}, \quad (2)$$

where $dL_{sp} = \frac{dA(\theta, \phi)}{\Delta T v_{sp}(\theta, \phi)}$,

and $dA(\theta, \phi) = d\theta d\phi \sin(\theta)$ is the local area. Equation 2 determines spreading length by dividing the local area dA by a distance of spreading perpendicular to the ridge axis, given by $\Delta T v_{sp}(\theta, \phi)$. Because each spreading ridge produces isochrons on either side of its axis, in the absence of subduction the integration of Equation 2 over all seafloor of age t yields double the ridge length at that time. The destruction of isochrons by subduction, however, causes measured values of $L_{sp}(t)$ to generally decrease with increasing seafloor age.

Average rates of spreading, V_{sp} , can be determined for times in the past by taking the length-weighted average of the local half-spreading rate along an isochron:

$$V_{sp}(t) = \frac{1}{L_{sp}(t)} \int_{T(\theta, \phi) = t - \Delta T/2}^{T(\theta, \phi) = t + \Delta T/2} v_{sp}(\theta, \phi) dL_{sp}, \quad (3)$$

where dL_{sp} is the local spreading length given by Equation 2 and v_{sp} is given by Equation 1. This length-weighted determination of average half-spreading rate is preferable to an area-weighted average because it avoids the over-weighting of fast-spreading seafloor inherent to area weighting. Thus, V_{sp} from Equation 3 is an estimate of the average half-spreading rate along the length of a former ridge at time t . Note that this estimate of spreading rate is determined only along the preserved length of the former spreading ridge, which, because of subduction, represents an increasingly smaller fraction of the original spreading length for older seafloor. Thus, estimates of V_{sp} become

increasingly uncertain for past times because they are based on a progressively smaller fraction of the original spreading length.

CENOZOIC AND CRETACEOUS TECTONIC CHANGE

Using half-spreading rates determined from Müller et al.'s (1997) data set (Fig. 1), we used Equation 3 to measure average half-spreading rates as a function of time both globally and for each of the eight ocean basins defined in Figure 1. To remove nonphysical slow spreading associated with transform faults, we do not include half-spreading rates slower than 15% of the average present-day spreading rate for a given basin (Fig. 2), as measured by taking the length-weighted average of full spreading rates given by DeMets et al. (1990). We find that this 15% cutoff removes nonphysical slow spreading rates associated with transform faults without eliminating spreading associated with past lithosphere production. For the present day, the average spreading rates measured from the Müller et al. (1997) age grid (Fig. 2, lines) generally are within the DeMets et al. (1990) error estimates for present-day seafloor spreading. Given that similar uncertainty is likely associated with rates measured from the Müller et al. (1997) age grid (which also rely on picks of seafloor magnetic anomalies), we take the favorable comparison of these two measurements of present-day seafloor spreading as a verification of the robustness of our method. For past times the range of uncertainty is at least as large as that shown for the present day.

Average half-spreading rates (Fig. 2) describe the tectonic evolution of each basin's spreading systems as a function of time. The global average of half-spreading rates (Fig. 2A) is

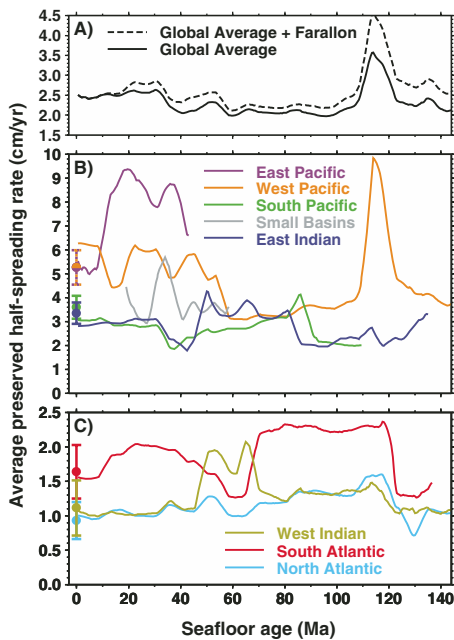


Figure 2. Average half-spreading rates (colored lines) calculated as function of seafloor age by applying Equation 3 to half-spreading map of Figure 1, using a 5 m.y. running mean ($\Delta T = 5$ m.y.). A: Global averages, both with and without subducted Farallon plate (see text). B: Averages for five basins (Fig. 1) whose margins are dominated by subduction zones. C: Averages for three basins (Fig. 1) surrounded by passive margins. Computed rates for present day compare favorably to independent estimates of present-day spreading determined by taking length-weighted averages of spreading rate estimates, shown as dots with error bars, taken from DeMets et al. (1990). Because spreading rates depend directly on the time scale used to assign ages to isochrons, we have applied the Cande and Kent (1995) time scale, which was used by Müller et al. (1997), to the DeMets et al. (1990) data, which slows rates by a factor of 0.957. Because DeMets et al. (1990) gave full spreading rates across ridges, orange and purple dots and error bars in part B are determined from spreading rates for combined East and West Pacific basins. Thus, this curve should be compared to the average of East and West Pacific curves slightly weighted toward the East Pacific curve because of its longer present-day ridge length (Fig. 1).

~2.1 cm/yr during the Late Cretaceous and early Cenozoic. Between ca. 40 Ma and ca. 30 Ma, the global average increased by ~20%, to ~2.5 cm/yr. This global increase was caused by accelerating spreading rates in the West Pacific basin, rates that almost doubled during this time (Fig. 2B). The West Pacific increase is likely the result of eastward motion of the Pacific-Farallon ridge system, which caused a Cenozoic increase in the age, and thus weight, of slabs subducting along the northern and western margins of the Pacific (Parsons, 1982). We (Conrad and Lithgow-Bertelloni, 2004) showed

that the resulting increase in the slab pull force drove faster Pacific plate motion, and thus faster Pacific spreading rates.

Spreading rates in basins with passive margins (Fig. 2C) remained fairly stable during the Cenozoic, exhibiting variations of only a few millimeters per year (Fig. 2C). The rate changes that occur generally have a tectonic explanation. For example, the West Indian basin shows an ~50% increase in spreading rate between ca. 65 Ma and ca. 50 Ma (Fig. 2C). This period of rapid spreading may be related to a strong slab pull force on the Indian plate, which was eliminated when India collided with Eurasia ca. 50 Ma or earlier. South Atlantic spreading was slower during this period (Fig. 2C), and can be explained by changes in African plate motion.

RIDGE LENGTHS AND LITHOSPHERE PRODUCTION RATES

Estimates of total lithosphere production rate require knowledge of ridge length as well as spreading rate. We calculate the length of preserved isochrons in each ocean basin using Equation 2 and find that preserved spreading lengths generally increase toward the present day (Fig. 3). This trend is expected because older seafloor is more likely to have been subducted since the time of its formation. We cannot directly measure isochron lengths for seafloor that has been subducted, but we can infer these lengths if (assumed symmetric) spreading counterparts are preserved. This is the case for the Pacific, where the Kula and Farallon plates, which dominated the northern and eastern Pacific for most of the Cenozoic, have been largely subducted beneath North America and South America. These plates were separated from the Pacific plate by a ridge system that produced most of the Cenozoic lithosphere of the Pacific plate (West Pacific basin). If we assume symmetrical spreading, we can estimate spreading lengths for the subducted Farallon plate by examining isochrons that are preserved on the Pacific side of the ridge.

To obtain a minimum estimate of subducted Farallon spreading length, we subtract the East Pacific spreading length from its counterpart in the West Pacific basin (Fig. 3). For ages younger than ca. 10 Ma, Cocos-Nazca spreading (Fig. 1) makes the East Pacific spreading lengths longer than those in the West Pacific, so we obtain zero contribution for the missing length (certainly an underestimate). For ages between ca. 10 and ca. 40 Ma, East Pacific lengths get smaller because they are lost to subduction, so our reconstruction of lost Farallon spreading grows to include a progressively larger fraction of the West Pacific spreading lengths. For ages older than ca. 40 Ma, Farallon subduction has eliminated all of the seafloor in the East Pacific, so our reconstructed Farallon spreading lengths equal the West Pacific spreading lengths. This reconstruction of subducted seafloor is conser-

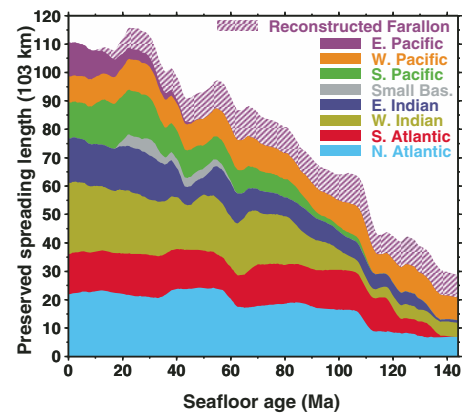


Figure 3. Total spreading length (isochron length), calculated using Equation 2 and $\Delta T = 5$ m.y., preserved on the seafloor of each basin, as a function of seafloor age. Lengths for subducted Farallon plate are estimated as described in text.

vative because in many instances (e.g., seafloor older than ca. 50 Ma beneath the Aleutians or young lithosphere beneath Central America), both sides of the ridge have been destroyed. For these situations our reconstruction does not recover spreading from either side of the ridge. Thus, our estimate of Farallon spreading lengths (Fig. 3) represents only a fraction of the total spreading length at the time. Nevertheless, adding reconstructed Farallon spreading lengths to the global summation (Fig. 3) shows that spreading lengths have decreased by at least ~5000 km (~4.5%) during the past 20 m.y.

We can obtain a minimum estimate of past rates of lithosphere production by multiplying preserved ridge lengths (Fig. 3) by rates of spreading (Fig. 2) for each basin. The result (Fig. 4) is analogous to the plot of seafloor area produced per unit age as a function of age. Except for our use of a 5 m.y. running mean, Figure 4 reproduces the area-age distribution

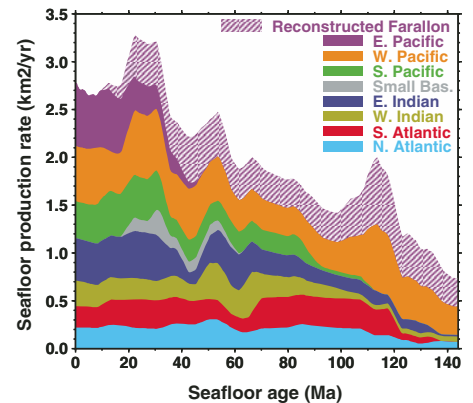


Figure 4. Net seafloor production rate for each basin as a function of age, calculated by multiplying the average half-spreading rates (Fig. 2) by the total spreading lengths (Fig. 3) for each basin, and reconstructed Farallon plate.

of Rowley (2002), who used its approximately triangular nature to infer nearly constant rates of lithosphere production by ridges. When past production of the Farallon lithosphere is added (Fig. 4), however, it becomes evident that lithospheric production rates were higher in the past. To determine Farallon production rates, we multiplied spreading rates from the West Pacific basin (Fig. 2B) with the reconstructed Farallon spreading lengths (Fig. 3). In doing so, we assumed symmetrical spreading despite the fact that asymmetrical spreading is common in spreading environments (Müller et al., 1998) and is evident on the East Pacific Rise. However, spreading along the East Pacific rise is faster on the Nazca plate side of the ridge, and has been for at least 40 m.y. (Fig. 2), so our reconstruction is likely conservative. If the half-spreading rates for the current East Pacific seafloor, which are as much as ~50% faster than those for the West Pacific during 20–40 Ma, also applied to the portion of East Pacific (Farallon) spreading that has been lost to subduction, then the lithospheric production rates inferred for the subducted Farallon plate would be as much as ~50% larger than the estimate shown in Figure 4.

By introducing seafloor production inferred for the Farallon plate (Fig. 4), we see that seafloor production rates have decreased during the past 20 m.y. The average rate of decrease (~0.025 km²/yr/m.y.) is a minimum estimate because our assumptions certainly underestimate past spreading lengths and likely underestimate the half-spreading rates that applied to them. This ~18% decrease in the global rate of lithosphere production occurred in only 20 m.y., and at a rate comparable to estimates of the rate of decrease determined from rates of sea-level lowering (~0.024 km²/yr/m.y. over 80 m.y.) (Gaffin, 1987) or changes in subduction rate (~0.02 km²/yr/m.y. over 50 m.y.) (Engebretson et al., 1992). Our estimates indicate that, prior to ca. 30 Ma, the rate of seafloor production was lower than it is today (Fig. 4). Although this decreased production rate results partly from slower spreading rates in the early Cenozoic (Fig. 2A), some of this measured decrease is due to the loss of seafloor to subduction since that time.

DISCUSSION AND CONCLUSIONS

We have examined gradients in present-day seafloor ages to estimate both past ridge lengths and spreading rates during the Cretaceous and Cenozoic. Globally, the average spreading rate increased by ~20% during the first half of the Cenozoic (Fig. 2A) due primarily to a near doubling of Pacific plate speed (Fig. 2B). The global average spreading rate has decreased by ~12% during the second half of the Cenozoic (Fig. 2A). When we include an inference for subducted Farallon seafloor, we find that ridge

lengths have decreased by at least 4.5% since 20 Ma, primarily due to the subduction of the Farallon-Pacific ridge system beneath western North America. Because the lost spreading ridges included some of the world's fastest, the combination of slow decreases in both spreading rate and ridge length resulted in a net decrease in the global rate of lithosphere production by at least ~18% in the past 20 m.y. Using less conservative assumptions, production rates that were more than 25% faster at 20 Ma are possible. Additional subduction of seafloor prior to the mid-Cenozoic makes estimating earlier trends in seafloor production rate difficult. However, a faster seafloor production rate in the past is consistent with observations of increasing Mg/Ca ratio (Hardie, 1996), decreasing sea level (Haq et al., 1987), and decreasing atmospheric carbon (Berner and Kothavala, 2001) during the Cenozoic, all of which can be attributed to decreasing lithosphere production rates. We show that this decrease occurred because the rapidly spreading Pacific-Farallon ridge system decreased in length during the Cenozoic.

Our results contrast strongly with Rowley's (2002) suggestion that lithosphere production rates have not significantly changed from their current rate during the past 180 m.y. Instead, a conservative reconstruction of isochrons for the subducted Farallon plate shows that production rates were at least ~18% higher (3.3 km²/yr; Fig. 4) and possibly as much as 25% larger (3.5 km²/yr if we assume East Pacific spreading rates for the subducted Farallon plate), as recently as 20 Ma (cf. 2.8 km²/yr for the present day [Fig. 4]; see also Rowley [2002]). In addition, given that a simple reconstruction of the Farallon plate led to the discovery of faster lithosphere production in the recent past, additional reconstruction of subducted seafloor may show even faster lithosphere production rates prior to ca. 30 Ma. Rapid spreading associated with the now-subducted Pacific-Kula and Kula-Farallon spreading systems may have driven additional crustal production in the earlier Cenozoic and Cretaceous.

Demicco (2004) showed that the approximately triangular nature of the present-day area/age versus age curve does not necessarily require constant lithosphere production rates, as suggested by Parsons (1982) and advocated by Rowley (2002). We have shown that varying rates of seafloor production, combined with changing ridge geometries, seem to have produced the approximately triangular distribution observed for the present day. Given the Cenozoic and Mesozoic history of changing plate geometries, spreading rates, and ridge lengths, and the fact that plate motions represent the surface expression of vigorous and time-dependent mantle flow, it is not surprising that lithosphere production rates vary significantly with time.

ACKNOWLEDGMENTS

We thank R. Demicco for a helpful review, and an anonymous reviewer for extensive comments that improved the analysis and discussion; financial support was provided by the David and Lucile Packard Foundation and National Science Foundation grants EAR-0609590 and EAR-0609553.

REFERENCES CITED

- Berner, R.A., and Kothavala, Z., 2001, GEOCARB III: A revised model of atmospheric CO₂ over Phanerozoic time: *American Journal of Science*, v. 301, p. 182–204.
- Cande, S.C., and Kent, D.V., 1995, Revised calibration of the geomagnetic polarity timescale for the Late Cretaceous and Cenozoic: *Journal of Geophysical Research*, v. 100, p. 6093–6095.
- Cogné, J.P., and Humler, E., 2004, Temporal variations of oceanic spreading and crustal production rates during the last 180 My: *Earth and Planetary Science Letters*, v. 227, p. 427–439.
- Conrad, C.P., and Lithgow-Bertelloni, C., 2004, The temporal evolution of plate driving forces: Importance of “slab suction” versus “slab pull” during the Cenozoic: *Journal of Geophysical Research*, v. 109, p. B10407, doi: 10.1029/2004JB002991.
- DeMets, C., Gordon, R.G., Argus, D.F., and Stein, S., 1990, Current plate motions: *Geophysical Journal International*, v. 101, p. 425–478.
- Demicco, R.V., 2004, Modeling seafloor-spreading rates through time: *Geology*, v. 32, p. 485–488.
- Engebretson, D.C., Kelley, K.P., Cashman, H.J., and Richards, M.R., 1992, 180 Million years of subduction: *GSA Today*, v. 2, p. 93–95.
- Gaffin, S., 1987, Ridge volume dependence on seafloor generation rate and inversion using long-term sea-level change: *American Journal of Science*, v. 287, p. 596–611.
- Haq, B.U., Hardenbol, J., and Vail, P.R., 1987, Chronology of fluctuating sea levels since the Triassic: *Science*, v. 235, p. 1156–1167.
- Hardie, L.A., 1996, Secular variation in seawater chemistry: An explanation for the coupled secular variation in the mineralogies of marine limestones and potash evaporites over the past 600 m.y.: *Geology*, v. 24, p. 279–283.
- Kominz, M.A., 1984, Oceanic ridge volume and sea-level change—An error analysis, *in* Schlee, J.S., ed., *Interregional unconformities and hydrocarbon accumulation*: American Association of Petroleum Geologists Memoir 36, p. 109–127.
- Müller, R.D., Roest, W.R., Royer, J.-Y., Gahagan, L.M., and Sclater, J.G., 1997, Digital isochrons of the world's ocean floor: *Journal of Geophysical Research*, v. 102, p. 3211–3214.
- Müller, R.D., Roest, W.R., and Royer, J.-Y., 1998, Asymmetric sea-floor spreading caused by ridge-plume interactions: *Nature*, v. 396, p. 455–459.
- Parsons, B., 1982, Causes and consequences of the relation between area and age of the ocean floor: *Journal of Geophysical Research*, v. 87, p. 289–302.
- Rowley, D.B., 2002, Rate of plate creation and destruction: 180 Ma to present: *Geological Society of America Bulletin*, v. 114, p. 927–933.

Manuscript received 24 February 2006
 Revised manuscript received 10 August 2006
 Manuscript accepted 28 August 2006

Printed in USA